The Journal of Neuroscience, December 1, 2000, *20*(23):8677–8684

Dopamine D_3 Receptors Expressed by All Mesencephalic Dopamine Neurons

Jorge Diaz,[1] Catherine Pilon,[2] Bernard Le Foll,[2] Claude Gros,[2] Antoine Triller,[3] Jean-Charles Schwartz,[2] and Pierre Sokoloff[2]

[1]*Laboratoire de Physiologie, Université René Descartes, 75006 Paris, France,* [2]*Unité de Neurobiologie et Pharmacologie Moléculaire (Institut National de la Santé et de la Recherche Médicale U 109), Centre Paul Broca, 75014 Paris, France, and* [3]*Biologie Cellulaire de la Synapse Normale et Pathologique (Institut National de la Santé et de la Recherche Médicale U 497), Ecole Normale Supérieure, 75230 Paris, France*

A polyclonal antibody was generated using synthetic peptides designed in a specific sequence of the rat D_3 receptor (D_3R). Using transfected cells expressing recombinant D_3R, but not D_2 receptor, this antibody labeled 45–80 kDa species in Western blot analysis, immunoprecipitated a soluble fraction of [^{125}I]iodosulpride binding, and generated immunofluorescence, mainly in the cytoplasmic perinuclear region of the cells. In rat brain, the distribution of immunoreactivity matched that of D_3R binding, revealed using [^{125}I]R(+)*trans*-7-hydroxy-2-[*N*-propyl-*N*-(3′-iodo-2′-propenyl)amino] tetralin ([^{125}I]7-*trans*-OH-PIPAT), with dense signals in the islands of Calleja and mammillary bodies, and moderate to low signals in the shell of nucleus accumbens (AccSh), frontoparietal cortex, substantia nigra (SN), ventral tegmental area (VTA) and lobules 9 and 10 of the cerebellum. Very low or no signals could be detected in other rat brain regions, including dorsal striatum, or in D_3R-deficient mouse brain. Labeling of perikarya of AccSh and SN/VTA appeared with a characteristic punctuate distribution, mostly at the plasma membrane where it was not associated with synaptic boutons, as revealed by synaptophysin immunoreactivity. In SN/VTA, D_3R immunoreactivity was found on afferent terminals, arising from AccSh, in which destruction of intrinsic neurons by kainate infusions produced a loss of D_3R binding in both AccSh and SN/VTA. D_3R-immunoreactivity was also found in all tyrosine hydroxylase (TH)-positive neurons observed in SN, VTA and A8 retrorubral fields, where it could represent D_3 autoreceptors controlling dopamine neuron activities, in agreement with the elevated dopamine extracellular levels in projection areas of these neurons found in D_3R-deficient mice.

Key words: nucleus accumbens shell; substantia nigra; ventral tegmental area; D_3 receptor-deficient mice; tyrosine hydroxylase; synaptophysin

Converging pharmacological, genetic and human postmortem studies have implicated the D_3 receptor (D_3R) in the physiopathology and treatment of schizophrenia, drug addiction and depression (Pilla et al., 1999; Lammers et al., 2000; Schwartz et al., 2000). In rat brain, the largest D_3R expression densities occur in granule cells of the islands of Calleja and in medium-sized spiny neurons of the rostral and ventromedial shell of nucleus accumbens (AccSh), which coexpress the D_1 receptor and neuropeptides (Diaz et al., 1994; Diaz et al., 1995; Le Moine and Bloch, 1996). The neurons from AccSh receive their dopaminergic innervation from the ventral tegmental area (VTA) and other innervations from cerebral cortex, hippocampus and amygdala (Zahm and Brog, 1992; Pennartz et al., 1994), project indirectly to entorhinal and prefrontal cortice and subserve the control of emotion, motivation and reward (Willner and Sheel-Krüger, 1991).

One aspect of the localization and function of the D_3R that is still highly debated is its occurrence as an autoreceptor, regulating the activity of dopamine neurons. We originally proposed the existence of D_3 autoreceptors on the basis of the expression in substantia nigra (SN) and VTA of D_3R mRNA, which strongly decreases after lesion of dopamine neurons (Sokoloff et al., 1990). This lesion, however, also downregulates postsynaptic D_3R in AccSh (Lévesque et al., 1995), by deprivation of brain-derived neurotrophic factor (BDNF), an anterograde factor of dopamine neurons (Guillin et al., 1999). Hence the lesion-induced decrease in SN/VTA could reflect a similar process occurring in non-dopaminergic neurons.

Dopamine release (Tang et al., 1994) and synthesis (O'Hara et al., 1996) are inhibited by stimulation of the D_3R expressed in a transfected mesencephalic cell line and various agonists, with limited preference for the D_3R (Sautel et al., 1995), inhibits dopamine release, synthesis and neuron electrical activity (for review, see Levant, 1997), giving support to the existence of D_3 autoreceptors. However, the selectivity of these agonists toward the D_3R *in vivo* is strongly questioned, because they elicit similar inhibition of dopamine neuron activities in wild-type and D_3R-deficient mice (Koeltzow et al., 1998). In addition, dopamine autoreceptor functions are suppressed in D_2 receptor-deficient mice (Mercuri et al., 1997; L'hirondel et al., 1998). Nevertheless, dopamine extracellular levels in the nucleus accumbens (Koeltzow et al., 1998) and striatum (R. Gainetdinov and M. G. Caron, personal communication) are twice as high in D_3R-deficient as in wild-type mice, suggesting a control of dopamine neurons activity by the D_3R.

Direct confirmation of the role of the D_3R as an autoreceptor requires the demonstration of its occurrence in dopamine neurons, namely by using immunocytochemical methods. In fact, the antibodies directed against the D_3R reported so far generated immunolabeling that did not overlap distributions of D_3R mRNA and binding sites (Ariano and Sibley, 1994; Larson and Ariano, 1995; Khan et al., 1998), which questions their specificity. In the present study, we have generated a polyclonal antibody against the D_3R using sequence-specific peptides and assessed its specificity using recombinant receptors and D_3R-deficient mice and by comparison with D_3R binding. This antibody has then been used to examine cellular localizations of the D_3R by comparison with tyrosine hydroxylase (TH) and synaptophysin immunoreactivities.

Received June 23, 2000; revised Aug. 29, 2000; accepted Aug. 30, 2000.

This work was supported by a grant from the European Commission (FP5 Programme QLG4-CT-1999-00075).

Correspondence should be addressed to Dr. Pierre Sokoloff, Unité de Neurobiologie et Pharmacologie Moléculaire (Institut National de la Santé et de la Recherche Médicale U 109), Centre Paul Broca, 2ter, rue d'Alésia, 75014 Paris, France. E-mail: sokol@broca.inserm.fr.

 0270-6474/00/208677-08$15.00/0

MATERIALS AND METHODS

Immunization, antiserum titration and antibody purification. The immunization procedure conformed with local guidelines and has been performed by a person accredited by the French Minister of Agriculture (decree 87848). The peptide H-YGAGMSPVERTRNSL-OH (Y15L) was coupled by copulation with diazotized benzidine to bovine serum albumin (BSA) and subcutaneously injected together with complete Freund's adjuvant once, and then with the incomplete Freund's adjuvant each week for 4 weeks (268 μg of peptide per injection), into female New Zealand rabbits. A booster injection in complete Freund's adjuvant was performed one month latter with the same immunogen. The peptide Y15L was coupled to keyhole Limpet hemocyanin and used for a booster injection (500 μg of the peptide) 3 months later. Three months later, the rabbits were injected with the peptide H-GAGMSPVERTRNSLY-OH (G15Y) coupled by copulation via bisdiazobenzidine to ovalbumin. Five booster injections with the latter peptide (350 μg of peptide/injection) were made during the 3 years that followed. Rabbits were bled every 1–4 weeks and serum titer was assayed using [^{125}I]tyrosyl-labeled G15Y or Y15L and polyethyleneglycol precipitation.

The best titer antiserum collected at the end of the immunization procedure was precipitated with ammonium sulfate, filtered on DEAE-Sephadex and immunopurified on a HiTrap column (Amersham Pharmacia Biotech, Little Chalfont, UK) coupled to peptide G15Y by the amino group. The purified antibody was eluted in glycine-HCl 0.1 M, pH 2.3.

Western blot analysis. Wild-type and transfected Chinese hamster ovary (CHO) cells expressing the D_2 receptor or D_3R (Sokoloff et al., 1990) were scrapped, harvested in 50 mM sodium phosphate buffer (PB) containing 150 mM NaCl (PBS), and homogenized in Tris-HCl buffer, 10 mM containing 5 mM EDTA and protease inhibitors (aprotinin, 1 μg/ml; leupeptin, 1 μg/ml; pepstatin, 0.1 μg/ml). Membranes were isolated by centrifugation at 5000 × *g* for 10 min and solubilized in PAGE-loading buffer (50 mM Tris-HCl, pH 7.4, 5 mM EDTA, 10% glycerol, 2% SDS, protease inhibitors as above). Proteins (20 μg) were separated by electrophoresis in 12% SDS-polyacrylamide gel and electrophoretically transferred to nitrocellulose filters. Blots were blocked in PBS Blotto (Pierce, New York, NY) with 1% bovine serum albumin at room temperature for 2 hr. The blots were then incubated with purified anti-D_3R antibody (1:2000) overnight at 4°C. After three 10 min washes in PBS containing 0.05% Tween 20, blots were incubated with a horseradish peroxydase-conjugated goat anti-rabbit γ-globulins antibody (1:10,000, Pierce) for 1 hr at room temperature and developed using the enhanced chemiluminescence procedure (Amersham Pharmacia Biotech).

Receptor immunoprecipitation. Membranes of CHO cells expressing the D_2 receptor or D_3R were solubilized in 1% digitonin, 1% sodium cholate, and 1 M NaCl in 50 mM sodium phosphate buffer, pH 7.4, for 30 min at 4°C, diluted twice in sodium phosphate buffer, and centrifuged for 30 min at 50,000 × *g*. Supernatants (100 μl) diluted 10 times in sodium phosphate buffer were incubated in a final volume of 400 μl with diluted preimmune serum or antiserum and [^{125}I]iodosulpride (0.1 nM, 2200 Ci/mmol) (Amersham) overnight at 4°C. Some incubations were performed with the antibody previously presaturated overnight with the peptide G15Y (1 μg/μl), and some were performed in the presence of 1 μM emonapride to measure nonspecific binding. Fifty microliters of a 50% (v/v) suspension of protein A-Sepharose (Amersham Pharmacia Biotech) were added, and tubes were incubated under gentle agitation for 2 hr at 4°C and then centrifuged for 3 min at 14,000 rpm. Aliquots of supernatants were filtered through GF/B filters coated with 0.3% polyethyleneimine, and filters were rinsed with 3 × 3 ml of cold sodium phosphate buffer. In preliminary experiments, this procedure allowed us to solubilize and recover up to 20% of membrane-bound receptors.

Animals, tissue, and cell preparation for immunohistochemistry and immunofluorescence. Male Wistar rats (180–250 gm, Iffa-Credo, L'Arbresles, France) or mice (see below) were anesthetized deeply with pentobarbital (30 mg/kg, i.p.) and then perfused transcardially with 50 ml of saline solution (0.9% NaCl warmed at 37°C), followed by 600 ml of an ice-cooled fixative solution containing 2% paraformaldehyde in 0.1 M PB, pH 7.5. The brains were removed, post-fixed in 2% paraformaldehyde for 1–2 hr at 4°C, and rinsed in PB solutions. Some brains were transferred into ascending series of sucrose solutions (10% overnight, 15% for 24 hr, and 20% for 24 hr), frozen and stored at −70°C, and then sectioned in coronal and sagittal planes with a cryostat in 30 μm sections. Other brains were immediately cut in the same planes with a vibratome in 40 μm sections that were collected, cryoprotected in PB containing 30% sucrose, and freeze-thawed (−75°C) to improve penetration of the antibodies. Cryostat or vibratome sections were collected in 0.05 M Tris buffer, pH 7.5, containing 150 mM NaCl (TBS) and then treated with blocking serum (5% normal donkey serum, 0.4% BSA, 0.1% gelatin, and 0.1% Tween 20 in TBS) for 1 hr at room temperature. CHO cells were cultured on 20 × 20 mm collagen-coated slides, rinsed with PBS, fixed for 30 min in 2% paraformaldehyde, rinsed again in 0.1 M glycine–PBS, and immersed in the blocking serum as above.

Detection of D_3R immunoreactivity by the immunoperoxidase method. The sections were incubated for 24–48 hr at room temperature with the immunopurified anti-D_3 receptor antibody diluted 1:2000 in TBS containing 5% normal donkey serum and 0.05% Tween 20 (TBS–NDST20). Some sections were incubated with the antibody previously presaturated overnight with the peptide G15Y (1 μg/μl). The sections were rinsed (four times for 10 min) in TBS containing 0.1% gelatin and 0.05% Tween 20 (TBS–GT20) and immersed for either 1–2 hr at room temperature or overnight at 4°C in biotinylated donkey anti-rabbit γ-globulins (Amersham) diluted 1:200 in TBS–NDST20. The sections were rinsed (three times for 10 min) in TBS–GT20 and then incubated for 1 hr at room temperature in avidin–biotin–HRP complex (ABC reagent, Vectastin-Elite; Vector Laboratories, Burlingame, CA). After rinsing in TBS containing Tween 20 (0.05%) and then in TBS, peroxidase activity was revealed by incubation with 3,3′ diaminobenzidine for 10–30 min at 4°C in the presence of hydrogen peroxide using the Sigma Fast diaminobenzidine tablets (Sigma, St. Louis, MO). The peroxidase reaction was stopped by several rinses in Tris-HCl. The sections were mounted on glass slides, dehydrated in graded ethanols, cleared, and then mounted in Acrytol for observation under a Zeiss Axiophot microscope.

Immunofluorescence experiments. Vibratome coronal sections taken at levels of both basal forebrain (nucleus accumbens–ventral pallidum) and midbrain (VTA–SN) regions were incubated for 24–48 hr at room temperature in a mixture of primary immunoreagents diluted in TBS–NDST20. The mixture consisted of purified anti-D_3R antibody diluted 1:2000 and mouse monoclonal antibodies directed against either synaptophysin (diluted 1:50) (Boehringer Mannheim Biochemica, Mannheim, Germany) or anti-TH (diluted 1:10,000) (Incstar, Stillwater, MN). Slides with fixated CHO cells were incubated for 48 hr at 4°C with the purified anti-D_3R antibody only, diluted 1:2,000. After four washes (10 min each) in TBS–GT20, the sections were incubated in FITC–donkey anti-mouse (Jackson Immunoresearch, West Grove, PA) diluted 1:200 in TBS–NDST20, followed by Cy3–donkey anti-rabbit γ-globulins (Jackson Immunoresearch), diluted 1:1000 in TBS–NDST20, for 1 hr at room temperature. To intensify the D_3R fluorescent immunostaining, some double-labeling experiments were performed using a biotinylated donkey anti-rabbit IgG (1:200 in TBS–NDST20) followed by three washes (10 min each) and incubation for 1 hr in Cy3-streptavidin (0.5 μg/ml in TBS–T20). The sections were washed (three times for 10 min), mounted on Super Frost Plus slides, and then coverslipped using Vectashield mounting medium (Vector Laboratories) and nail polish to seal the coverslip. Sections were examined and photographed using Zeiss Plan-Neofluar objectives and band-pass filter sets for FITC and rhodamine. Control experiments were performed to ensure that each primary antibody did not react with the non-corresponding secondary antibody-conjugate. In such experiments, sections were incubated as follows: rabbit anti-D_3R antibody, followed by FITC–donkey anti-mouse or mouse anti-TH followed by Cy3–donkey anti-rabbit. In these controls, only light autofluorescence and no cross-reactive immunostaining were observed.

D_3R-deficient mice. Heterozygotous mice bearing a mutation invalidating the D_3R gene, originally obtained from S. Fuchs (Weizmann Institute, Rehovot, Israel) (Accili et al., 1996), were bred and mated. DNA was prepared from a piece of the tail (3–5 mm) using the DNAeasy tissue kit (Qiagen France, Courtaboeuf, France) and amplified with the mixture of primers GCA GTG GTC ATG CCA GTT CAC TAT CAG and CCT GTT GTG TTG AAA CCA AAG AGG AGA GG, amplifying the exon 3 of the wild-type D_3R, and TGG ATG TGG AAT GTG TGC GAG and GAA ACC AAA GAG GAG AGG GCA GGA C, amplifying the PGK cassette of the mutated gene. Agarose gel electrophoresis allowed us to detect homozygotous wild-type mice (a single band at 137 bp), homozygotous mutated mice (a single band at 200 bp), and heterozygotous mice (bands at 137 and 200 bp). Homozygotous mutated mice and their wild-type littermates were used in the study.

Lesion studies. Male Sprague Dawley rats (180–200 gm, Iffa Credo, L'Arbresles) were anesthetized with pentobarbital (50 mg/kg). Nucleus accumbens lesions were made by infusion of kainate (1.5 μl of a solution at 2.5 μg/ml in 25 mM Tris-HCl buffer, pH 7.4, at the following coordinates: anterior-posterior +1.7 mm; lateral −1 mm; ventral −7 mm from the dural surface. The infusion cannula was left in position for 3 min after each one-side infusion. Animals were killed 10 d after stereotaxic surgery. Assessment of the placement and extent of the lesion was performed under microscopic observation of Nissl-stained sections.

Receptor autoradiography. Unfixed 10 μm cryostat brain sections were preincubated at room temperature three times for 5 min in 50 mM sodium-HEPES buffer, pH 7.5, containing 1 mM EDTA and 0.1% BSA. They were incubated in the same buffer containing 0.2 nM [^{125}I]R(+)*trans*-7-hydroxy-2-[*N*-propyl-*N*-(3′-iodo-2′-propenyl)amino] tetralin ([^{125}I]*trans*-7-OH-PIPAT; 2200 Ci/mmol; Amersham) for 45 min at room temperature. Nonspecific binding was determined by incubating adjacent sections in the same medium in the presence of 1 μM dopamine. After incubation, slices were washed four times for 2 min in ice-cold sodium-HEPES buffer containing 100 mM NaCl, dipped in ice-cold distilled water, and then dried under a stream of cold air. Autoradiograms were generated by apposing sections to ^{3}H-Hyperfilm (Amersham) for 2–4 d and developed in D-19 developer. Autoradiographic signals were quantified on two to three slices per animal using an image analyzer (IMSTAR, Paris, France). Gray values were converted to microcuries per gram wet weight using ^{125}I standard stripes (Amersham).

In situ *hybridization.* The procedure has been described previously (Diaz et al., 1995). Briefly, paraformaldehyde-fixed slices (10 μm) were treated with proteinase K (1 μg/ml) and then with 0.25% acetic anhydride in triethanolamine buffer. The sections were hybridized with a ^{33}P-radiolabeled cRNA probe for D_3R mRNA (2×10^6 dpm per slide) in 65%

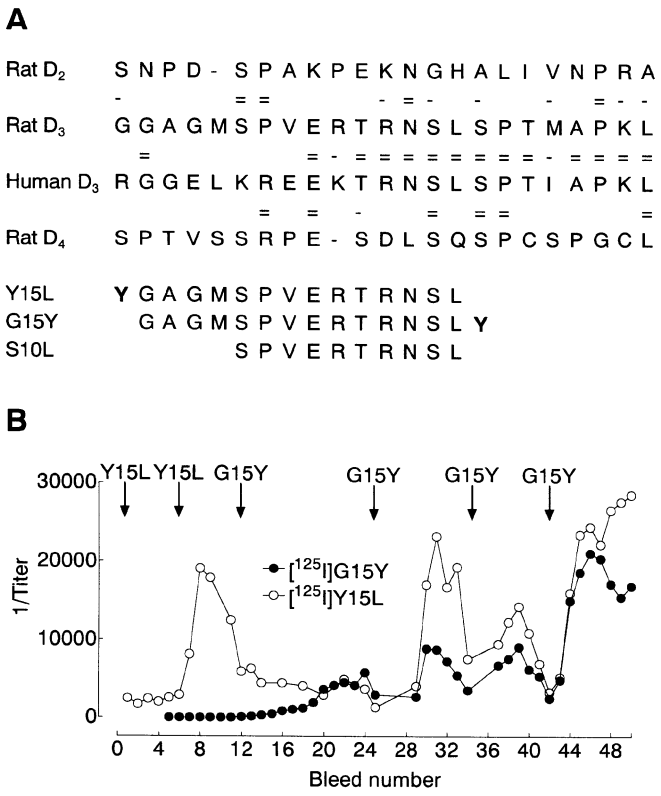

Figure 1. Generation of antibodies. *A,* Amino acid sequence alignments (single letter code) of dopamine D_2, D_3, and D_4 receptors and the peptides used in the study to generate antibodies. *B*, Generation of immunoreactivity against [^{125}I]-labeled peptides. A rabbit was immunized with peptides Y-15-L and G-15-Y injected at times indicated by *arrows*, and immunoreactivity in the serum was measured using [^{125}I]Y-15-L (○) or [^{125}I]G-15-Y (●). Immunoreactivity titer was the antiserum dilution giving 50% of maximal bound radioactivity (70–90% of total radioactivity in the assay), calculated from saturation curves established with four to six serial antiserum dilutions. Antisera were obtained from bleeding every 1–2 weeks.

deionized formamide, 10% dextran sulfate, 1× Denhardt's solution, 2× SSC, 0.1% sodium pyrophosphate, 100 μg/ml yeast tRNA, and 100 μg/ml denatured salmon sperm DNA. After incubation and rinsing, slices were treated with RNase A (200 μg/ml), washed and dehydrated through a graded series of ethanol, and apposed to films (Hyperfilm β-max, Amersham) for 1 month. Films were developed in D-19 developer (15°C) for 5 min, rinsed rapidly in deionized water, and fixed in 30% sodium thiosulfate for 10–20 min.

RESULTS

Generation of anti-D_3R antibodies

The immunizing peptide sequence was designed in the putative third intracytoplasmic loop of the rat D_3R, which has no homologies with the sequence of other dopamine receptor subtypes (Fig. 1*A*). A portion of this sequence has a strong homology with the human D_3R. A search in databases did not reveal any other homology with a known protein. A first peptide, Y15L, had an additional tyrosine residue at the N terminus, allowing coupling to the carrier tyrosines with diazotized benzidine, and was used to immunize rabbits. After the initial immunization and a booster injection, rabbits were subsequently boosted with a second peptide, G15Y, having the same sequence, but with the additional tyrosine used for coupling located at the C terminus instead of the N terminus. Immunoreactivity of the antisera was measured with the two peptides [^{125}I]-labeled at either the C or N terminus (Fig. 1*B*). Although immunoreactivity against [^{125}I]Y15L raised and reached a similar antiserum titer after each booster injection, immunoreactivity against [^{125}I]G15Y appeared only after G15Y injections, and its titer increased progressively thereafter. At the end of immunization, antisera titers were similar against the two iodinated peptides. Furthermore, antibodies had similar affinities for Y15L and G15Y (EC_{50} = 0.5 nM; data not shown), as well as a shorter peptide S10L (see sequence on Fig. 1*A*), indicating that antibodies indeed recognized internal epitopes.

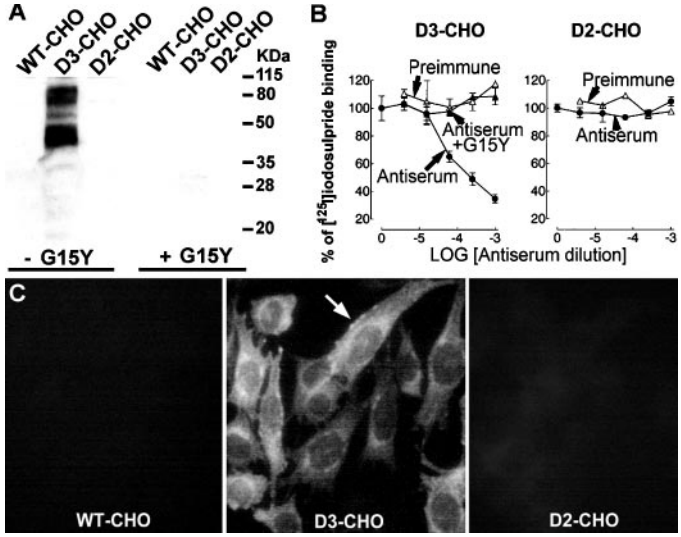

Figure 2. The antibody recognizes the recombinant D_3R expressed in transfected cells. *A*, Western blot of crude membrane proteins of wild-type CHO cells (*WT-CHO*) or CHO cells expressing the D_3R (*D3-CHO*) or the D_2 receptor (*D2-CHO*) with the purified antibody without (*−G15Y*) or with (*+G15Y*) presaturation with the immunizing peptide G15Y. *B*, Immunoprecipitation of [^{125}I]iodosulpride binding sites solubilized from membranes of CHO cells expressing the D_3R (*left*) but not the D_2 receptor (*right*). Receptors solubilized and labeled with [^{125}I]iodosulpride were incubated in the presence of antiserum or preimmune serum in increasing dilutions, in the presence or absence of G-15-Y peptide. Receptor-antibody complexes were then precipitated with protein A-Sepharose beads, and the nonprecipitated receptors were assayed in the supernatant. *C*, D_3R immunofluorescence in wild-type CHO cells (*left*) or CHO cells expressing the D_3R (*middle*) or the D_2 receptor (*right*). Note the labeling at the plasma membrane of D_3R-expressing cells (*arrow*). No signal could be detected when the first antibody was omitted (data not shown).

Characterization of antibodies using recombinant dopamine receptors

In crude membrane preparations of CHO cells expressing the D_3R that were subjected to SDS-PAGE, the immunopurified antibody labeled major bands at ~45 and ~80 kDa (Fig. 2*A*). Minor bands, possibly corresponding to degraded proteins, were also visible at ~60 kDa and below 35 kDa. All of these bands were absent when the antibody was presaturated with the immunizing peptide G15Y. No signal could be detected with membranes from wild-type or D_2 receptor-expressing CHO cells.

D_3 or D_2 receptors expressed by CHO cell lines were solubilized with a digitonin–cholate mixture and labeled with [^{125}I]iodosulpride in the presence of antiserum or preimmune serum. The activity in the supernatant was measured after precipitation of antibody-receptor complexes with immobilized protein A. As shown in Figure 2*B*, the antiserum immunoprecipitated >60% of solubilized D_3R, but not D_2 receptor, and the effect was abolished by presaturation of the antibody with the immunizing peptide. Because the antiserum had no effect on [^{125}I]iodosulpride binding without protein A (<5% inhibition at any dilution starting from 10^{-3}; data not shown), the depletion of [^{125}I]iodosulpride binding in the supernatant of protein A precipitation represented true immunoprecipitation.

Strong immunofluorescence signals generated with an immunopurified antibody were detected on D_3R-expressing CHO cells, but not on wild-type nor D_2 receptor-expressing CHO cells (Fig. 2*C*). Most of the signal appeared in the cytoplasm of D_3R-expressing cells, particularly in the perinuclear region, but some cells also displayed immunofluorescence at the plasma membrane (Fig. 2*C*, *arrow*). No signal could be detected when the D_3R antibody was

omitted or presaturated with the immunizing peptide (data not shown).

Distribution of D_3 receptor immunoreactivity in rat and wild-type or D_3 receptor-deficient mouse brains

In rat brain slices, there was a close overlap between the distributions of D_3R immunoreactivity, revealed by immunoperoxidase, and binding sites for [^{125}I]*trans*-7-OH-PIPAT, a D_3R-selective ligand (Burris et al., 1994). Thus, highest immunoreactivity levels were found in the islands of Calleja (Fig. 3*B*), which also express the highest density of D_3R mRNA (Bouthenet et al., 1991; Diaz et al., 1995). Strong labeling was also observed in AccSh. A much weaker signal was observed in the core of nucleus accumbens (Fig. 3*B*), a region where D_3R mRNA and binding levels are weak (Fig. 3*A*) (Bouthenet et al., 1991; Diaz et al., 1995). In normal $D_3R^{+/+}$ mouse brain, the D_3R immunolabeling was similar to that found in rat brain and undetectable in D_3R-deficient mouse brain (Fig. 3*D*,*E*).

A semiquantitative comparison between D_3R immunoreactivity, binding, and mRNA levels in rat brain (Table 1) shows an overall agreement between distributions of the three markers. For instance, a high level of D_3R immunoreactivity was found in mammillary bodies, a region expressing high levels of D_3R binding and mRNA (Bouthenet et al., 1991), whereas a much weaker signal was observed in dorsolateral striatum, where the latter markers are hardly detectable. Moderate signals were observed in the frontoparietal cortex, ventral pallidum, anteroventral thalamic nucleus, and lateral habenula, which also express D_3R binding (Table 1), whereas other brain regions contained very low or undetectable levels of both D_3R immunoreactivity and binding. The only discrepancy was found in the cerebellum, where high levels of D_3R binding and mRNA are present in lobules 9 and 10 (Bouthenet et al., 1991; Diaz et al., 1995), whereas weaker D_3R immunoreactivity was observed (Table 1). This suggested that the D_3R may differ in cerebellum and other brain regions, but cDNAs amplified from mRNAs extracted from cerebellar lobules 9 and 10 and from nucleus accumbens had identical sequences, notably in the region corresponding to the immunizing peptide (data not shown).

D_3 receptor immunoreactivity in the mesencephalon

Moderate D_3R immunoreactivity, revealed by the immunoperoxidase method, was found in the rat SN/VTA complex, where individual cell bodies were clearly visualized in all parts of the complex (Fig. 3*H*,*J*). Enlargement shows labeling of individual cell bodies in the SN pars compacta (Fig. 3*J*). The immunoreactivity was abolished by presaturation of the antibody with the immunizing peptide G15Y (Fig. 3*I*,*K*). In contrast, [^{125}I]*trans*-7-OH-PIPAT binding was prominent in a restricted part of the complex, at the junction between SN pars compacta and VTA (Fig. 3*F*), and did not overlap the highest D_3R mRNA densities (Fig. 3*G*). [^{125}I]*trans*-7-OH-PIPAT binding in this area indeed labeled the D_3R, because this binding was completely absent in D_3R-deficient mice (Fig. 4*A*,*B*). D_3R immunoreactivity, revealed by the immunoperoxidase method in SN/VTA, was largely absent in D_3R-deficient mice (Fig. 4*C*,*D*), and the characteristic punctuate distribution of D_3R immunofluorescence in neurons of VTA was completely absent in these mice (Fig. 4*E*,*F*). In addition, D_3R immunoreactivity, binding, and mRNA were present in the A8 retrorubral dopamine cell group in the rat (Table 1).

To investigate the possibility that a fraction of D_3R binding in SN/VTA was present on afferent fibers from extrinsic neurons, we performed lesions of neurons intrinsic to AccSh by local infusions of kainate. Ten days later, this lesion elicited disappearance of Nissl-stained cells centered in the shell part of nucleus accumbens, but extended to the core part of nucleus accumbens and medioventral striatum (data not shown). No signs of *trans*-synaptic degeneration were observed: intrinsic neurons present in SN/VTA were apparently normal in number and shape (data not shown). The lesion elicited large and identical decreases (−62 and −63%, respectively) in D_3R binding in both the lesioned area and ipsilateral SN/VTA (Fig. 5*A*,*B*).

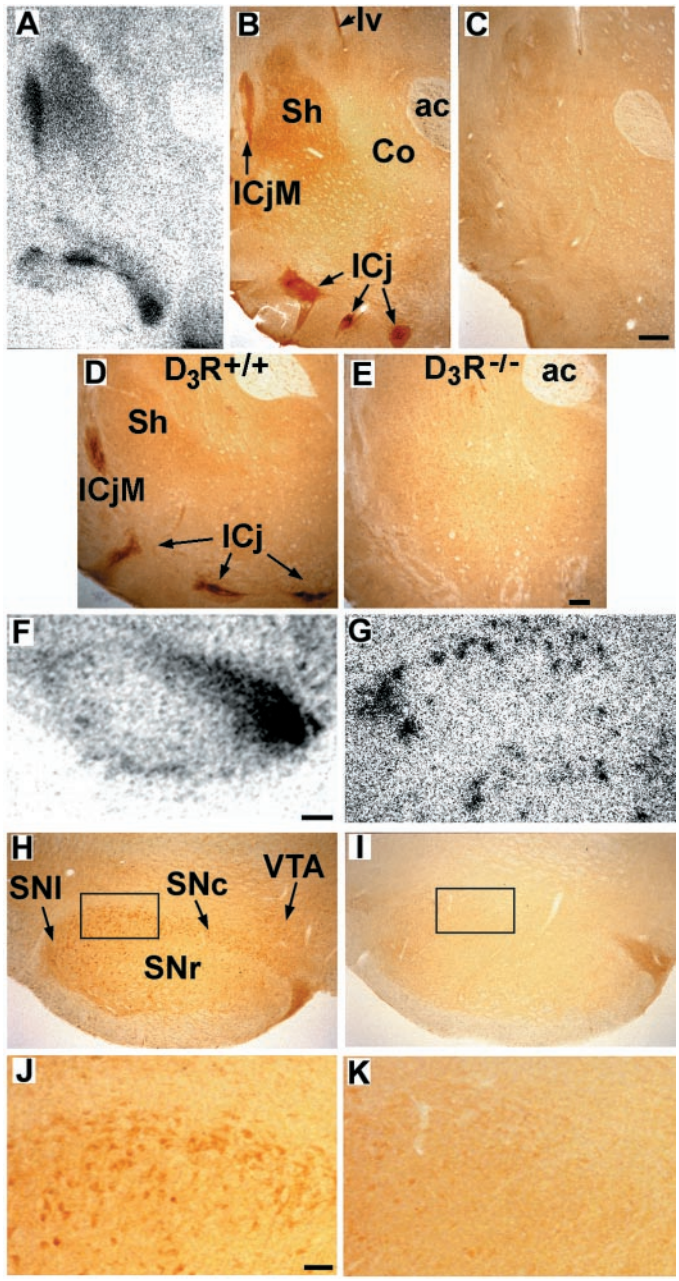

Figure 3. Comparisons of D_3R binding (*A*, *F*), D_3R immunoreactivity (*B–E*, *H–K*), and D_3R mRNA (*G*) in brain slices of rat (*A–C*, *F–K*), $D_3R^{+/+}$ (*D*), or $D_3R^{-/-}$ (*E*) mice. D_3R binding sites were labeled with the selective D_3R radioligand [^{125}I]7-*trans*-OH-PIPAT, and immunoreactivity was revealed using diaminobenzidine and D_3R mRNA by *in situ* hybridization with a [^{33}P]-labeled riboprobe. In *C*, *I*, and *K*, the antibody was presaturated with the peptide G15Y. *A–E* show micrographs taken at the level of the ventral part of the striatal complex and *F–K* at the level of SN and VTA. In ventral striatum, [^{125}I]7-OH-PIPAT binding (*A*) and D_3R immunoreactivity (*B*) overlap; D_3R immunoreactivity was absent in $D_3R^{-/-}$ mice (*E*). In SN/VTA, [^{125}I]7-OH-PIPAT binding (*F*) was prominent at the junction between SN pars compacta (*SNc*) and VTA, whereas D_3R mRNA (*G*) was enriched in the lateral part of SN (*SNl*) and present in cells of the SN pars reticulata (*SNr*), SNc, and VTA. D_3R immunoreactivity (*H*) was present in cells and fibers of SNl, SNc, SNr, and VTA. *J* and *K* are enlargements of the rectangles in *H* and *I*, respectively, showing individual labeled cell bodies in the SNc in *J*. *ac*, Anterior commissura; *Co*, nucleus accumbens core; *ICj*, islands of Calleja; *ICjM*, island of Calleja major; *lv*, lateral ventricle; *Sh*, nucleus accumbens shell. Scale bars: *A–C*, *F–I*, 0.5 mm; *D*, *E*, 0.1 mm; *J*, *K*, 125 μm.

Comparison of D_3 receptor and tyrosine hydroxylase immunofluorescences

To assess the occurrence of D_3 autoreceptors, double-labeling experiments with antibodies directed against the D_3R and TH were

Table 1. Compared distributions of D_3 receptor mRNA, binding, and immunoreactivity in rat brain structures

Brain region	D_3R mRNA[a]	D_3R binding[b]	D_3R–IR[c]
Frontoparietal cortex	+	+/++	++
Frontal cortex	+/−	+	+
Nucleus accumbens shell	++	++	++
Nucleus accumbens core	+	+	+
Islands of Calleja			
Granule cells	+++	++	++
Hilar region	+/−	+++	+++
Ventromedial striatum	+	+	+
Ventrolateral septum	+/−	+	+
Dorsal striatum	0	+/−	+/−
Ventral pallidum	+	++	++
Medial mammillary bodies	+++	+++	+++
Lateral mammillary bodies	0	0	0
Lateral hypothalamus	0	+	+
Anteroventral thalamic nucleus	+	++	++
Lateral habenula	+/−	++	++
Hippocampus	+/−	+/−	+/−
Ventral tegmental area	+/−	+	+
Substantia nigra pars reticulata	+/−	+/−	+
Substantia nigra pars compacta	+/−	++	+
Substantia nigra pars lateralis	+	+/−	+/−
A8 retrorubral field	+	+	+
Cerebellum (lobules 9 and 10)			
Purkinje cells	+++	+/−	+
Molecular layer	0	+++	++

[a]Data from Bouthenet et al. (1991) and Diaz et al. (1995).

[b]Data obtained with [^{3}H]7-OH-DPAT from Diaz et al. (1995) or with [^{125}I]*trans*-7-OH-PIPAT (present study).

[c]D_3R immunoractivity.

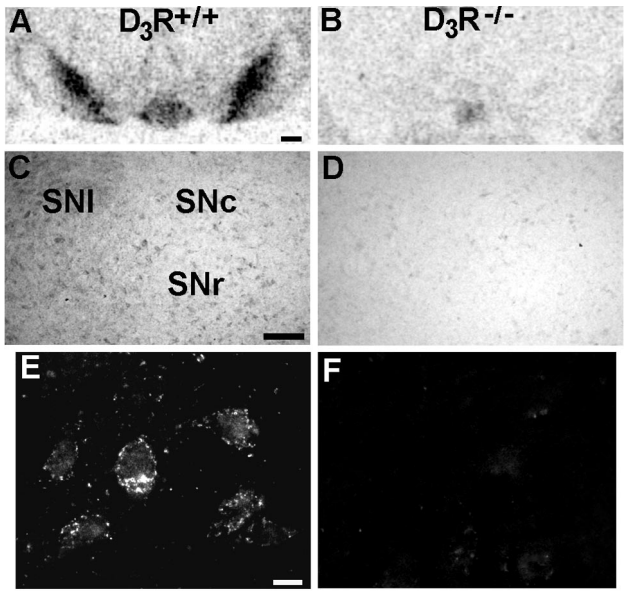

Figure 4. D_3R binding (*A*, *B*), immunoperoxidase (*C*, *D*), and immunofluorescence (*E*, *F*) in SN/VTA of $D_3R^{+/+}$ (*A*, *C*, *E*) and $D_3R^{-/-}$ (*B*, *D*, *F*) mice. *E* and *F* show photomicrographs taken in the VTA. Note that the punctuate immunoreactivity is absent in $D_3R^{-/-}$ mice. *SNc*, SN pars compacta; *SNl*, SN pars lateralis; *SNr*, SN pars reticulata. Scale bars: *A*, *B*, 0.2 mm; *C*, *D*, 100 μm; *E*, *F*, 10 μm.

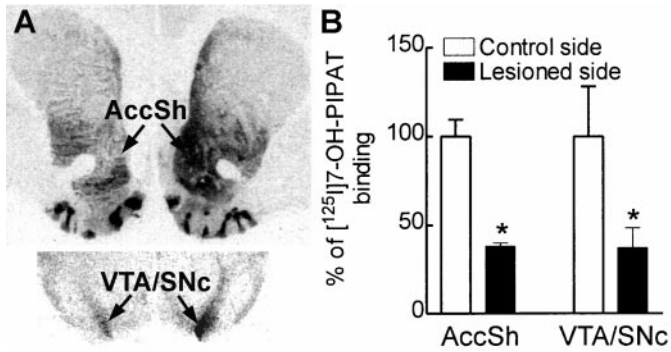

Figure 5. Loss of D_3R binding in both AccSh and VTA/SN 10 d after an infusion of kainate into the left nucleus accumbens. Sections in *A* show [^{125}I]7-OH-PIPAT binding at the level of the nucleus accumbens (*top*) and mesencephalon (*bottom*). *B*, Sections similar to those shown in *A* and obtained from four animals were analyzed by densitometry. $^*p < 0.03$ by the two-tailed Mann–Whitney *U* test.

performed on sections containing SN/VTA or AccSh, a region of dopamine neurons projection where the D_3R is abundant. In SN/VTA, D_3R immunofluorescence corresponded to the immunoreactivity revealed with the immunoperoxidase method (Figs. 3*H*, 6*A*). At lower magnification (Fig. 6*A*,*B*), distributions of D_3R and TH immunofluorescences were overlapping in the SN pars compacta and VTA but not in SN pars reticulata and SN pars lateralis, where most D_3R-positive cells were TH negative. Microscopic examination of every section from 10 animals (15–20 sections per animal) at high magnifications (see representative examples in Fig. 6*C-F*) indicated that all TH-positive cells also displayed D_3R immunofluorescence; we could not find any TH-positive cell not expressing D_3R immunofluorescence in SN and VTA. In contrast, some D_3R-positive cells (a few of them are designated by *arrows* in Fig. 6*D*) did not display TH immunofluorescence. At the highest magnification used (Fig. 6*E*,*F*), there were clearly distinct cellular localizations of the two immunofluorescences: D_3R immunofluorescence appeared with a characteristic punctuate distribution at the plasma cell membrane and within the cytoplasm, whereas TH immunofluorescence was homogeneously distributed in the cytoplasm. Both immunofluorescences were absent from the cell nucleus. In addition, on a limited number of sections ($n = 3$) taken at the level of the retrorubral A8 dopamine cell group, we also observed that all TH-positive cells also displayed D_3R immunofluorescence (data not shown).

In AccSh, D_3R immunofluorescence also appeared with a punctuate distribution at the plasma membrane of cell bodies and within the neuropil (Fig. 6*G*). TH immunofluorescence was mainly distinct from D_3 receptor immunofluorescence, with very rare apparent coincidences (Fig. 6*H*).

Comparison of D_3 receptor and synaptophysin immunofluorescences

To assess whether the D_3R immunofluorescence was localized at the vicinity of synaptic components, we compared distributions of D_3R and synaptophysin immunofluorescences in AccSh (Fig. 6*I*), islands of Calleja (Fig. 6*J*), and VTA (Fig. 6*K*). The punctuate distribution of D_3R immunofluorescence both in the cell bodies, mostly near the plasma membrane, and in the neuropil in the three regions did not correspond to the distribution of synaptophysin immunofluorescence, and only few apparent coincidences could be found.

DISCUSSION

Many studies have used antibodies raised against carrier-coupled synthetic peptides, the sequence of which is chosen in unique and predicted antigenic regions of the target protein. The antibodies raised in this manner are likely to recognize mainly the free, not the coupled, extremity of the peptide, which is a valuable strategy

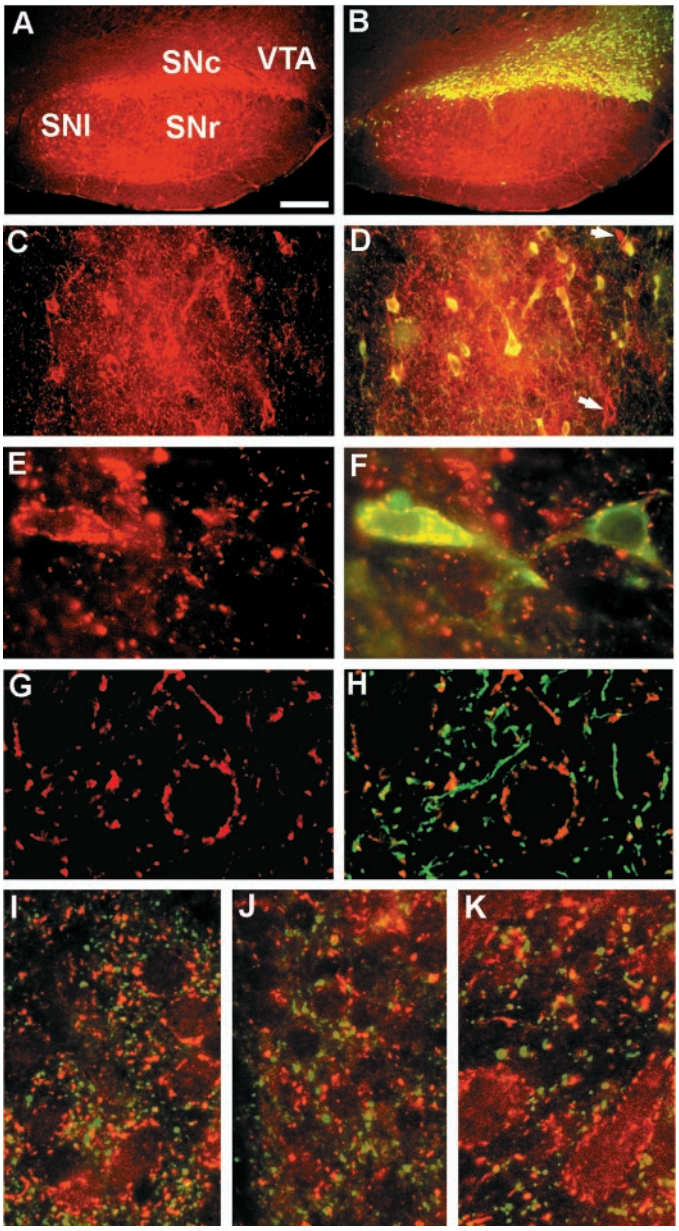

Figure 6. Comparison of D_3R and TH and synaptophysin immunofluorescences in rat brain. *A*, *C*, *E*, and *G* show D_3R immunofluorescence alone (Cy3, *red*). *B*, *D*, *F*, and *H* show double-labeling immunofluorescence of D_3R (Cy3, *red*) and TH (FITC, *green*). *A* and *B* show pictures obtained in the whole SN/VTA complex. *C* and *D* show pictures taken at the level of the junction between SNc and VTA. Neurons expressing D_3R but not TH immunofluorescence are marked by *arrows*. *E* and *F* show neurons in the VTA. *G* and *H* are taken at the level of the nucleus accumbens. *I–K* show double labeling immunofluorescence of D_3R (Cy3, *red*) and synaptophysin (FITC, *green*). *I*, *J*, and *K* show photomicrographs taken at the level of the nucleus accumbens shell, islands of Calleja, and VTA, respectively. In the three regions, D_3R immunofluorescence has a punctuate distribution at the plasma cell membrane, which segregates in cellular components distinct from those containing synaptophysin. *SNc*, SN pars compacta; *SNl*, SN pars lateralis; *SNr*, SN pars reticulata. Scale bars: *A*, *B*, 1 mm; *C*, *D*, 125 μm; *E*, *F*, 25 μm; *G*, *H*, 10 μm; *I–K*, 15 μm.

if the chosen sequence is at the N or C termini of the target protein, but a possible drawback if the sequence is internal. In the case of the D_3R, the N-terminal sequence has several putative sites for N-glycosylation, which may hinder recognition of the native protein, and the C terminus displays significant homologies with D_2 and D_4 receptor corresponding sequences. Hence, we decided to generate antibodies by using a synthetic peptide taken at the level of the third intracytoplasmic loop, coupled to the carrier by its N terminus, and then using a peptide having the same sequence but coupled by its C terminus. As expected, this strategy indeed favored generation of antibodies recognizing internal epitopes, because these antibodies display similar titer and affinity for the immunizing peptides, whether they are [^{125}I]tyrosyl-labeled at the C or N terminus. The immunopurified antibody also binds to denatured as well as native recombinant D_3R expressed by transfected CHO cells. The major immunoreactive species are ~40 and 80 kDa in size, and the smallest species may correspond to a degraded, incompletely synthesized, or nonglycosylated form (M_r 45,500 Da deduced from the predicted amino acid sequence), whereas the largest species may correspond to either SDS and reduction-resistant dimers or glycosylated forms. The species at ~80 kDa have the same apparent size as D_2/D_3 receptor binding sites labeled with photoaffinity radioligands using brain tissue homogenates (Amlaiky and Caron, 1985; Redouane et al., 1985), suggesting the largest as the active form. This hypothesis needs confirmation, however, because we could not reliably measure the apparent size of the native D_3R from rat brain, which is not surprising given its very low expression level: 10–100 times lower than that of the D_2 receptor (Lévesque et al., 1992).

Thus, in transfected CHO cells, the overexpressed D_3R recognized by the antibody is largely present as immature or degraded protein, which is in agreement with its main occurrence in the cytoplasm, particularly in the perinuclear region of the cell. This cellular localization markedly contrasts with that found in neurons, where the D_3R is apparently mainly present at the plasma membrane, with only few occurrences as cytoplasmic patches, probably associated with recycling or synthesizing vesicles. In addition, the antibody recognizes recombinant solubilized D_3R, in an active form able to bind a radioligand and precipitable by immobilized protein A. This antibody would therefore be a valuable tool for studying the D_3R regulation, e.g., phosphorylation.

In rat brain sections, the pattern of immunolabeling matched that of D_3R binding and transcripts, with highest levels present in the islands of Calleja and mammillary bodies, moderate to low levels in AccSh, frontoparietal cortex, lobules 9 and 10 in cerebellum, and SN/VTA, and very low levels in other brain structures including striatum. The observation that immunolabeling and D_3R binding patterns overlap is a strong criterion for assessing the specificity of this antibody, which was apparently not fulfilled in previous studies. In the latter, the specificity of the antibodies used was questionable because highest levels of alleged D_3R-like immunoreactivity were not found in AccSh or islands of Calleja but in striatum and core of nucleus accumbens (Ariano and Sibley, 1994) or in hippocampus (Khan et al., 1998), which contains low or undetectable levels of D_3R binding or mRNA. The selectivity of the antibody developed herein is also based on the solid evidence, lacking in previous studies, that the immunolabeling it generates is absent in D_3R-deficient mice. This antibody therefore appears to have the specificity required for reliable immunocytochemistry.

The only minor discrepancy identified so far is the lowest level of immunolabeling in lobules 9 and 10 of the cerebellum, as compared with D_3R binding and mRNA. Because we have presently confirmed that the D_3R in the cerebellum has a sequence identical to that found in the nucleus accumbens, this apparent mismatch could be because of an inappropriate tissue preparation, leading to a loss of accessibility of the antibody or antigenicity in this particular brain area. D_3R binding is present in dendritic trees of Purkinje cells of the cerebellar molecular layer (Diaz et al., 1995), which may not be totally preserved by the fixatives. Alternatively, the D_3R in the cerebellum could partly be in a form not recognized by the antibody. The sequence of the immunizing peptide contains a putative site for casein kinase 2 (S/T-X-X-D/E), a protein kinase very abundant in brain (Blanquet, 2000). Phosphorylation by this or a similar enzyme activity at this site may hinder recognition by the antibody.

The antibody developed in the present study allowed us to not only confirm the localization of the D_3R in rat brain but also to address the important issue of its occurrence as an autoreceptor. Three distinct kinds of immunolabeling localization were found in

SN/VTA that most likely correspond to the D_3R, because the immunolabeling herein is absent in D_3R-deficient mice. The first is expressed by non-dopaminergic neurons, which are the most abundant in the SN pars lateralis and also contain the highest levels of D_3R mRNA. This suggests that a large fraction of D_3R gene transcripts are expressed by non-dopaminergic neurons, which may be liable to downregulation of D_3R expression after dopamine neuron denervation by 6-hydroxydopamine (Sokoloff et al., 1990), similar to that occurring in the nucleus accumbens (Lévesque et al., 1995) as a result of BDNF deprivation (Guillin et al., 1999). It remains to be determined whether the putative downregulation of D_3R expression in non-dopaminergic mesencephalic neurons after dopamine neuron ablation also results from the loss of BDNF, as is the case of striatal neurons (Guillin et al., 1999), or from the loss of another factor. BDNF and its receptor trkB are expressed in mesencephalon (Altar et al., 1994; Seroogy et al., 1994), together with other neurotrophic factors (Fallon and Loughlin, 1995).

The second localization of D_3R immunolabeling in SN/VTA most likely corresponds to presynaptic heteroreceptors present on terminals of neurons originating from AccSh. Such a pathway has been identified by tract-tracing experiments (Berendse et al., 1992). In agreement, we found that a lesion by kainate of accumbal neurons decreased D_3R binding to a similar extent in AccSh and SN/VTA. This indicates that the D_3R in this latter area is mainly present on afferent terminals.

In SN, VTA, and the A8 retrorubral field, we found a third localization of D_3R immunoreactivity in all dopamine neurons observed, which were identified as TH-positive neurons. This observation is at variance with our previous double *in situ* hybridization studies (Diaz et al., 1995), which allowed us to detect only a few neurons expressing both tyrosine hydroxylase and D_3R mRNAs. In fact, long exposure of photographic emulsion after *in situ* hybridization with a D_3R mRNA probe produced weak but distinct signals evenly distributed within cells of SN/VTA (J. Diaz, unpublished results), in agreement with the occurrence of D_3 autoreceptors in all dopamine neurons and the higher sensitivity of double immunofluorescence compared with double *in situ* hybridization.

In dopamine neurons, as in postsynaptic neurons in AccSh, D_3R immunoreactivity appears distinct from cytoplasmic TH immunoreactivity, with a striking punctuate distribution along the plasma membrane, not overlapping synaptophysin immunoreactivity. The D_3R therefore appears not to be present in the vicinity of synaptic boutons, and very rare apparent co-occurrences of D_3R and TH immunoreactivities were noticed in fibers of both SN/VTA and AccSh. This result suggests that the D_3R is mainly extrasynaptic, like the D_1 and D_2 receptors (Yung et al., 1995), and that dopamine acts through the D_3R at some distance of its releasing sites, i.e., in a paracrine manner suggested previously (Diaz et al., 1995). This situation is not exceptional for neuromodulators, because other examples exist, e.g., for serotonin (Bunin and Wightman, 1999) or neurotensin (Boudin et al., 1998). Insofar as the sensitivities of immunofluorescence detection at nerve terminals and perikarya are identical, the results also imply that D_3 autoreceptors are rather somatodendritic, but confirmation of this localization requires the use of higher resolution methods.

In agreement with the selective somatodendritic localization of D_3 autoreceptors, the inhibitory control of dopamine release by nerve terminals seems to be exerted exclusively by D_2 autoreceptors (L'hirondel et al., 1998). D_3 autoreceptors, together with D_2 autoreceptors (Mercuri et al., 1997), may thus rather control the electrical activity of dopamine neurons, which would explain the elevated extracellular dopamine in projection areas of these neurons in D_3R-deficient mice. This control could have been masked in experiments using compounds inadequately selective of the D_3R (Koeltzow et al., 1998), because the compounds used also activate the D_2 receptor. Alternatively, D_3 autoreceptors could not be operant in anesthetized animals or *in vitro* in brain slices used in electrophysiological studies (Mercuri et al., 1997; Koeltzow et al., 1998), whereas elevated dopamine extracellular levels were measured in freely moving D_3R-deficient mice. Finally, D_3 autoreceptors may mediate yet unrecognized control of other dopamine neuron activities, such as synthesis or release of neuropeptides coexpressed with dopamine in these neurons, e.g., neurotensin, cholecystokinin, or neurotrophins.

REFERENCES

Accili D, Fishburn CS, Drago J, Steiner H, Lachowicz JE, Park B-H, Gauda EB, Lee EJ, Cool MH, Sibley DR, Gerfen CR, Westphal H, Fuchs S (1996) A targeted mutation of the D_3 receptor gene is associated with hyperactivity in mice. Proc Natl Acad Sci USA 93:1945–1949.

Altar CA, Siuciak JA, Wright P, Ip NY, Lindsay RM, Wiegand SJ (1994) *In situ* hybridization of *trk*B and *trk*C receptor mRNA in rat forebrain and association with high-affinity binding of [^{125}I] BDNF, [^{125}I] NGF-4/5 and [^{125}I] NT-3. Eur J Neurosci 6:1389–1405.

Amlaiky N, Caron MG (1985) Photoaffinity labeling of the D2-dopamine receptor using a novel high affinity radioiodinated probe. J Biol Chem 260:1983–1986.

Ariano MA, Sibley DR (1994) Dopamine receptor distribution in the rat CNS: elucidation using anti-peptide antisera directed against the D_{1A} and D_3 subtypes. Brain Res 649:95–110.

Berendse HW, Groenewegen HJ, Lohman AHM (1992) Compartmental distribution of ventral striatal neurons projecting to the mesencephalon in the rat. J Neurosci 12:2079–2103.

Blanquet PR (2000) Casein kinase 2 as a potentially important enzyme in the nervous system. Prog Neurobiol 60:211–246.

Boudin H, Pélaprat D, Rostène W, Pickel VM, Beaudet A (1998) Correlative ultrastructural distribution of neurotensin receptor proteins and binding sites in the rat substantia nigra. J Neurosci 18:8473–8484.

Bouthenet M-L, Souil E, Martres M-P, Sokoloff P, Giros B, Schwartz J-C (1991) Localization of dopamine D_3 receptor mRNA in the rat brain using in situ hybridization histochemistry: comparison with D_2 receptor mRNA. Brain Res 564:203–219.

Bunin MA, Wightman RM (1999) Paracrine neurotransmission in the CNS: involvement of 5-HT. Trends Neurosci 22:377–382.

Burris KD, Filtz TM, Chumpradit S, Kung MP, Foulon C, Hensler JG, Kung HF, Molinoff PB (1994) Characterization of [^{125}I](R)-*trans*-7-hydroxy-2-[*N*-propyl-*N*-(3′-iodo-2′-propenyl)amino] tetralin binding to dopamine D_3 receptors in rat olfactory tubercle. J Pharmacol Exp Ther 268:935–942.

Diaz J, Lévesque D, Griffon N, Lammers CH, Martres M-P, Sokoloff P, Schwartz J-C (1994) Opposing roles for dopamine D_2 and D_3 receptors on neurotensin mRNA expression in nucleus accumbens. Eur J Neurosci 6:1384–1387.

Diaz J, Lévesque D, Lammers CH, Griffon N, Martres M-P, Schwartz J-C, Sokoloff P (1995) Phenotypical characterization of neurons expressing the dopamine D_3 receptor. Neuroscience 65:731–745.

Fallon JH, Loughlin SE (1995) Substantia nigra. In: The rat nervous system (Paxinos G, ed), pp 215–237. San Diego: Academic.

Guillin O, Damier L, Griffon N, Diaz J, Carroll P, Schwartz J-C, Sokoloff P (1999) Role of brain-derived neurotrophic factor in the control of D_3 receptor expression. Eur J Neuropsychopharmacol 9:S184–S185.

Khan ZU, Gutierrez A, Martin R, Penafiel A, Rivera A, De La Calle A (1998) Differential regional and cellular distribution of dopamine D2-like receptors: an immunocytochemical study of subtype-specific antibodies in rat and human brain. J Comp Neurol 402:353–371.

Koeltzow TE, Xu M, Cooper DC, Hu XT, Tonegawa S, Wolf ME, White FJ (1998) Alterations in dopamine release but not dopamine autoreceptor function in dopamine D_3 receptor mutant mice. J Neurosci 18:2231–2238.

Lammers CH, Diaz J, Schwartz J-C, Sokoloff P (2000) Selective increase of dopamine D_3 receptor gene expression as a common effect of chronic antidepressant treatments. Mol Psychiatry 5:378–388.

Larson ER, Ariano MA (1995) D_3 and D_2 dopamine receptors: visualization of cellular expression patterns in motor and limbic structures. Synapse 20:325–337.

Le Moine C, Bloch B (1996) Expression of the D_3 dopamine receptor in peptidergic neurons of the nucleus accumbens: comparison with the D_1 and D_2 dopamine receptors. Neuroscience 73:131–143.

Levant B (1997) The D_3 dopamine receptor: neurobiology and potential clinical relevance. Pharmacol Rev 49:231–252.

Lévesque D, Diaz J, Pilon C, Martres M-P, Giros B, Souil E, Schott D, Morgat J-L, Schwartz J-C, Sokoloff P (1992) Identification, characterization and localization of the dopamine D_3 receptor in rat brain using 7-[^{3}H]-hydroxy-*N*,*N* di-n-propyl-2-aminotetralin. Proc Natl Acad Sci USA 89:8155–8159.

Lévesque D, Martres M-P, Diaz J, Griffon N, Lammers CH, Sokoloff P, Schwartz J-C (1995) A paradoxical regulation of the dopamine D_3 receptor expression suggests the involvement of an anterograde factor from dopamine neurons. Proc Natl Acad Sci USA 92:1719–1723.

L'hirondel M, Chéramy A, Gedeheu G, Artaud F, Saiardi A, Borrelli E, Glowinski J (1998) Lack of autoreceptor-mediated inhibitory control of

dopamine release in striatal synaptosomes of D_2 receptor-deficient mice. Brain Res 792:253–262.

Mercuri NB, Daiardi A, Bonci A, Picetti R, Calabresi P, Bernardi G, Borrelli E (1997) Loss of autoreceptor function in dopaminergic neurons form dopamine D_2 receptor-deficient mice. Neuroscience 79:323–327.

O'Hara CM, Uhland-Smith A, O'Malley KL, Todd RD (1996) Inhibition of dopamine synthesis by dopamine D_2 and D_3 but not D_4 receptors. J Pharmacol Exp Ther 277:186–192.

Pennartz CM, Groenewegen HJ, Lopes da Silva FH (1994) The nucleus accumbens as a complex of functionally distinct neuronal ensembles: an integration of behavioural, electrophysiological and anatomical data. Prog Neurobiol 42:719–761.

Pilla M, Perachon S, Sautel F, Garrido F, Mann A, Wermuth CG, Schwartz J-C, Everitt BJ, Sokoloff P (1999) Selective inhibition of cocaine-seeking behaviour by a partial dopamine D_3 receptor agonist. Nature 400:371–375.

Redouane K, Sokoloff P, Schwartz J-C, Hamdi P, Mann A, Wermuth CG, Roy J, Morgat J-L (1985) Photoaffinity labeling of D_2 dopamine binding subunits from rat striatum, anterior pituitary and olfactory bulb with a new probe, [^{3}H]azidosulpride. Biochem Biophys Res Commun 130:1086–1092.

Sautel F, Griffon N, Lévesque D, Pilon C, Schwartz JC, Sokoloff P (1995) A functional test identifies dopamine agonists selective for D_3 versus D_2 receptors. NeuroReport 6:329–332.

Schwartz J-C, Diaz J, Pilon C, Sokoloff P (2000) Possible implications of the D_3 receptor in schizophrenia and antipsychotic drug actions. Brain Res Rev 31:277–287.

Seroogy KB, KH L, Tran TMD, Guthrie KM, Isackson PJ, Gall CM (1994) Dopaminergic neurons in rat ventral midbrain express brain-derived neurotrophic factor and neurotrophin-3 mRNAs. J Comp Neurol 342:321–334.

Sokoloff P, Giros B, Martres M-P, Bouthenet M-L, Schwartz J-C (1990) Molecular cloning and characterization of a novel dopamine receptor (D_3) as a target for neuroleptics. Nature 347:146–151.

Tang L, Todd RD, O'Malley KL (1994) Dopamine D_2 and D_3 receptors inhibit dopamine release. J Pharmacol Exp Ther 270:475–479.

Willner P, Sheel-Krüger J (1991) The mesolimbic dopamine system: from motivation to action. Chichester: Wiley.

Yung KKL, Bolam JP, Smith AD, Hersch SM, Ciliax BJ, Levey AI (1995) Immunocytochemical localization of D_1 and D_2 dopamine receptors in the basal ganglia of the rat: light and electron microscopy. Neuroscience 65:709–730.

Zahm DS, Brog JS (1992) On the significance of subterritories in the "accumbens" part of the rat ventral striatum. Neuroscience 50:751–767.